Determinants of Substrate Specificity in the Superfamily of Amino Acid Dehydrogenases[†,‡]

Patrick J. Baker,[*,§,||] Maria L. Waugh,[§,||] Xing-Guo Wang,[⊥,#] Tim J. Stillman,[§] Andrew P. Turnbull,[§] Paul C. Engel,[⊥] and David W. Rice[§]

The Krebs Institute, Department of Molecular Biology and Biotechnology, The University of Sheffield, Western Bank, Sheffield S10 2TN, U.K., and Department of Biochemistry, University College Dublin, Belfield, Dublin 4, Ireland

Received August 14, 1997; Revised Manuscript Received October 8, 1997[⊗]

ABSTRACT: The subunit of the enzyme glutamate dehydrogenase comprises two domains separated by a cleft harboring the active site. One domain is responsible for dinucleotide binding and the other carries the majority of residues which bind the substrate. During the catalytic cycle a large movement between the two domains occurs, closing the cleft and bringing the C4 of the nicotinamide ring and the Cα of the substrate into the correct positioning for hydride transfer. In the active site, two residues, K89 and S380, make interactions with the γ-carboxyl group of the glutamate substrate. In leucine dehydrogenase, an enzyme belonging to the same superfamily, the equivalent residues are L40 and V294, which create a more hydrophobic specificity pocket and provide an explanation for their differential substrate specificity. In an attempt to change the substrate specificity of glutamate dehydrogenase toward that of leucine dehydrogenase, a double mutant, K89L,S380V, of glutamate dehydrogenase has been constructed. Far from having a high specificity for leucine, this mutant appears to be devoid of any catalytic activity over a wide range of substrates tested. Determination of the three-dimensional structure of the mutant enzyme has shown that the loss of function is related to a disordering of residues linking the enzyme's two domains, probably arising from a steric clash between the valine side chain, introduced at position 380 in the mutant, and a conserved threonine residue, T193. In leucine dehydrogenase the steric clash between the equivalent valine and threonine side chains (V294, T134) does not occur owing to shifts of the main chain to which these side chains are attached. Thus, the differential substrate specificity seen in the amino acid dehydrogenase superfamily arises from both the introduction of simple point mutations and the fine tuning of the active site pocket defined by small but significant main chain rearrangements.

The amino acid dehydrogenase superfamily has considerable commercial potential, both for the chiral synthesis of novel nonproteogenic amino acids for use in the pharmaceutical industry and also for use as diagnostic reagents to monitor the serum levels of amino acids which accumulate in a range of metabolic diseases. We are currently investigating the determinants of the differential substrate specificity in these enzymes in an attempt both to elucidate the molecular basis of this specificity and to try to engineer new enzymes which will act on novel substrates. This family of enzymes catalyzes the $NAD(P)^+$-linked oxidative deamination of L-amino acids to their corresponding α-keto acids, and sequence homology between these enzymes clearly indicates the presence of an enzyme superfamily related by divergent evolution (*1*−*3*). The members of this superfamily show distinct substrate specificities; glutamate dehydrogenase recognizes and binds glutamate in preference to all other amino acids (*4*), leucine and valine dehydrogenase will catalyze the oxidation of short, aliphatic amino acids only (*5*−*8*), and phenylalanine dehydrogenase has a marked preference for aromatic amino acids as substrate, although it will also accept smaller hydrophobic amino acids with reduced efficiency (*9*−*12*).

We have previously solved the atomic structures of two of the members of this enzyme superfamily, the glutamate dehydrogenase from *Clostridium symbiosum* (*13*, *14*) and the leucine dehydrogenase from *Bacillus sphaericus* (*15*). These two enzymes share a very similar subunit structure, as predicted on the basis of sequence similarity (*3*), with each subunit composed of two domains separated by a cleft harboring the active site. The site of NAD^+ binding has been identified for both enzymes, and in one crystal form of GluDH we have observed the substrate glutamate binding, which has suggested a possible reaction mechanism (*14*). The mode of NAD^+ binding, the design of the active site, and the catalytic chemistry are similar in both GluDH and LeuDH. However, there are significant differences in the residues which line the pocket into which the side chain of the amino acid substrate binds. In GluDH, the γ-carboxyl group of the glutamate substrate is anchored by interactions with Lys89 and Ser380, with the residues Gly90, Ala163, and Val377 forming interactions with the hydrophobic part of the side chain. In LeuDH these last three residues are fully conserved (Gly41, Ala113, and Val291, respectively), whereas Lys89 and Ser380 in GluDH become Leu40 and Val294 in LeuDH, making for a markedly more hydrophobic substrate side chain binding pocket. Despite the close

[†] This work was supported by the BBSRC, the Wellcome Trust, the European Union, and the New Energy Development Organisation.

[‡] The coordinates of the structure have been deposited with the Brookhaven Protein Data Bank, accession code 1AUP.

* To whom correspondence should be addressed (P.Baker@sheffield.ac.uk).

[§] The University of Sheffield.

[||] P.J.B. and M.L.W. contributed equally to this work.

[⊥] University College Dublin.

[#] Present address: Albert Einstein College of Medicine, 1300 Morris Park Ave., Bronx, NY 10461.

[⊗] Abstract published in *Advance ACS Abstracts,* December 1, 1997.

S0006-2960(97)02024-2 CCC: $14.00

similarity of the subunit structure in these two enzymes, intriguingly they form different quaternary assemblies. In GluDH six subunits assemble into a hexamer of 32 symmetry, whereas in LeuDH eight subunits assemble into an octamer in 42 symmetry.

The two substitutions in the side chain binding pocket from hydrophilic residues in GluDH to hydrophobic residues in LeuDH have been proposed to be the critical components of the differential substrate specificity in these two enzymes (*3*). To test this hypothesis a K89L,S380V double mutant of GluDH was engineered using site-directed mutagenesis, with the object of transforming the substrate specificity from glutamate toward leucine. As expected, this mutant GluDH showed dramatically decreased activity with glutamate as the substrate compared to the wild-type GluDH, with k_{cat}/k_M ratios of 5.0×10^3 s^{-1} M^{-1} and 4.1 s^{-1} M^{-1} for L-glutamate at pH 7.0 for the wild-type and mutant enzymes, respectively (*16*). However, tests with a range of other amino acids, including leucine, failed to reveal any significant level of enzymatic activity. We have therefore determined the three-dimensional structure of this double mutant in an attempt to explain why the predicted change in specificity did not occur, and this paper presents the results of that study.

EXPERIMENTAL PROCEDURES

The K89L,S380V double mutant of *C. symbiosum* GluDH was prepared and purified as described previously (*16*). Briefly, a mutant of the clostridial *gdh* gene in the bacteriophage M13mp19 vector was constructed using mismatched oligonucleotide primers and subcloned into the expression vector ptac85 and overexpressed in *Escherichia coli* strain Q100, grown in Luria−Bertani medium, supplemented with 100 μg/mL ampicillin. Harvested cells were sonicated and centrifuged, and the protein was purfied from the supernatant using a combination of gel filtration and ion-exchange columns. For crystallization, 10 μL drops of a solution containing 10 mg/mL K89L,S380V double mutant of *C. symbiosum* GluDH and 1.0 M sodium glutamate in 0.1 M potassium phosphate buffer, pH 7.3, were suspended over wells containing 0.1 M potassium phosphate buffer, pH 7.3, and 38−46% ammonium sulfate. Crystals of maximum dimensions $0.3 \times 0.3 \times 0.6$ mm grew within 4 weeks and were characterized as belonging to space group *R*32 with cell dimensions $a = 162.9$ Å and $c = 100.6$ Å and a monomer in the asymmetric unit. X-ray data to 2.5 Å were collected from a single crystal at room temperature on station PX9.5 of the Daresbury Synchrotron Radiation Service, using a MAR Research image plate, with rotations of 1.5° per image and an incident wavelength of 0.92 Å. The data were processed using MOSFLM (*17*), and all subsequent data reduction used programs from the CCP4 suite (*18*), unless otherwise stated. A total of 17 791 independent reflections were recorded, with an average redundancy of 5.1 and an *R*-factor of 0.07 (99% complete to 2.5 Å, Table 1a).

As the space group and cell dimensions of the mutant enzyme crystals were very similar to those of the glutamate-bound wild-type crystal form (*14*), it was envisaged that the arrangement of the molecules in the unit cell would be very similar, with a monomer in the asymmetric unit and the GluDH hexamer constructed from the crystallographic 3- and 2-fold axes. This was confirmed by molecular replacement using the structure of the closed form of GluDH as a search model, truncating the side chains of the two mutated residues to the β carbon and removing the coordinates for the bound glutamate and all water molecules. The highest peak on the cross-rotation function corresponded to values of $\omega = 0°$ and $\kappa = 0°$, and furthermore, a single peak of 17.9σ was seen in the translation function at fractional coordinates (0.002, 0.002, −0.002). The search model was subjected to rigid body refinement using TNT (*19*) first as one subunit and then as two domains at 6 Å resolution, followed by two-domain rigid body refinement at 4.5, 3.0, and finally 2.5 Å, which reduced the *R*-factor from 0.45 to 0.39. Positional and *B*-factor refinement further reduced the *R*-factor to 0.23. Cycles of rebuilding were then carried out using FRODO (*20*). The electron density for residues 185−208 and 383−399 in the initial $3|F_o| - 2|F_c|e^{-i\alpha calc}$ map was very broken, and indistinct and OMIT maps were calculated with these residues missing from the refined model. During the progress of refinement, density returned for the flanking regions and extra residues were added in this area. However, in the final map no density for residues 193−204 and 383−393 could be seen, and we must conclude that the polypeptide chain is disordered in these areas, rather than adopting a different conformation from the wild-type enzyme. The final model has an *R*-factor of 0.19 for all data in the resolution range 18−2.5 Å, a total of 3315 atoms (including 40 solvent molecules) with stereochemical parameters of rms bond deviations 0.017 Å, and rms bond angle deviations of 1.3° (Table 1b).

Table 1: Data Processing and Model Refinement Statistics

(a) Data Processing Statistics	
data set	K89L,S380V
no. of crystals	1
no. of measurements	90734
no. of independent reflections	17791
av $I/\sigma I$ (20.0−2.50 Å)	9.5
av $I/\sigma I$ (2.57−2.50 Å)	2.4
resolution	18−2.5 Å
completeness (20−2.5 Å)	99%
R_{merge}	0.07
(b) Refinement Statistics	
resolution range	18−2.5 Å
R-value (all data)	0.19
no. of reflections	17791
total non-H atoms	3315
solvent sites	40
B-value model	individual isotropic
av *B*-value	43.0 Å^2
rms deviations	
bonds	0.017 Å
angles	1.3°
trigonal groups	0.010 Å
planar groups	0.015 Å
Ramachandran outliers	none
residues missing from model	193−204; 383−393

RESULTS AND DISCUSSION

Fold of the Mutant Enzyme. The subunit of GluDH is divided into two domains, separated by a cleft, with each domain constructed from a central β sheet flanked by α helices. Six subunits assemble into a hexamer with 32 symmetry. Domain I is formed from the residues 1−200 and 431−449 and is responsible for self-assembly of the hexamer, with all the interactions around the 2-fold and 3-fold axes coming from residues in this domain. The other domain, domain II (residues 201−430), adopts a variant of

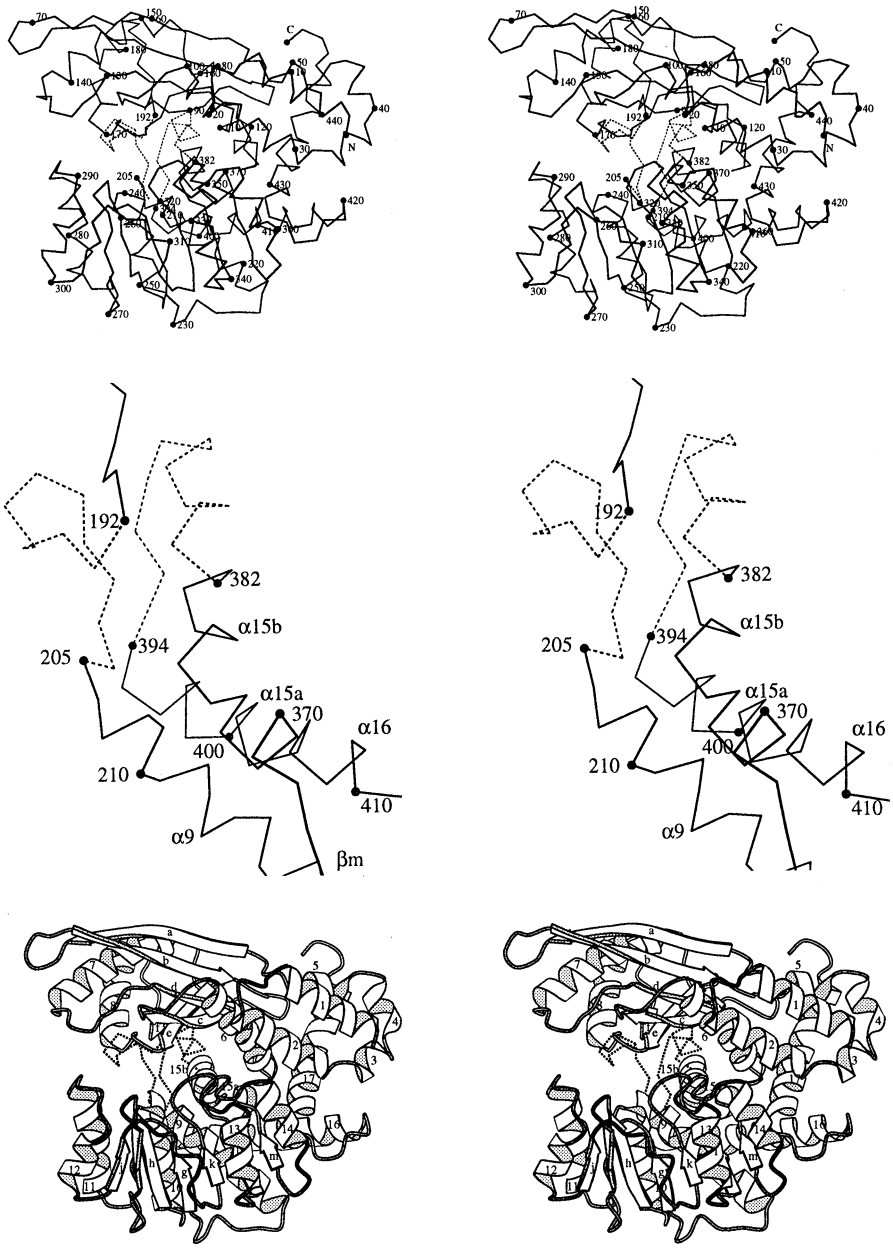

FIGURE 1: Three Molscript (*22*) stereo representations of a single subunit of the K89L,S380V double mutant GluDH, with the 3-fold axis of the hexamer vertical. (a, top) The Cα backbone, with every 10th residue shown as a black dot and labeled, (b, middle) a close-up of the domain interface, showing the disordered loops, and (c, bottom) a schematic drawing with the strands and helices labeled. In each case the disordered residues in the mutant structure are shown as a dashed line, in the position they occupy in the wild-type structure.

the common dinucleotide binding fold first described by Rossmann (*21*). In the wild-type enzyme the NAD^+ cofactor binds at the C-terminal end of the parallel β strands in this domain, lying in the cleft between the two domains. The glutamate substrate binds deep in the cleft, with the side chain of the glutamate lying in a pocket on the enzyme surface (*14*). As expected, on account of the mutation of the two residues that are critical for glutamate binding, and in spite of the presence of glutamate in the crystallization medium of the K89L,S380V mutant, no electron density could attributed to bound glutamate in this crystal form. In the mutant enzyme, residues 193−204 and 383−393 are disordered in the electron density map. In the wild-type structure these residues form strand βf and the loop to helix α9 and the latter part of helix α15b and the loop to α16, respectively. These two stretches of polypeptide lie in the domain interface and pack against each other in the structure. Apart from these residues, the polypeptide chain of the mutant adopts the same fold as the wild-type enzyme (Figure 1).

Domain Movement. We have previously solved two different crystal forms of *C. symbiosum* GluDH: one, the free enzyme in space group *C*2 (*13*), and the other, with glutamate bound, in space group *R*32 (*14*). In both crystal forms the domains I of the hexamer are in the same relative orientation with respect to each other and also with respect to the 32 symmetry point of the hexamer and form an invariant core. The domains II, however, which bind the dinucleotide, lie distant from the 32 symmetry point and make few interactions around the 2- or 3-fold axes (Figure 2). In each crystal form the positions of the domains II in the hexamer, relative to the domains I and the 32 symmetry point, are different, with the cleft between domain I and domain II being smaller in the crystals of the glutamate complex. This positional difference of the two domains in

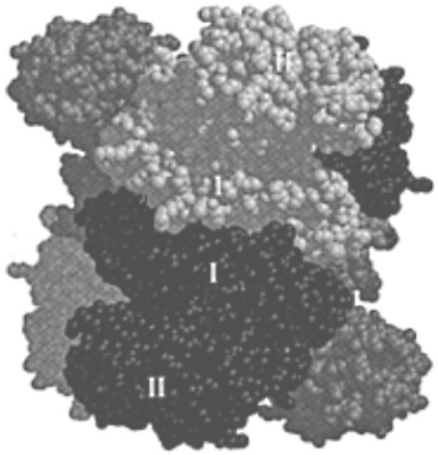

FIGURE 2: Schematic drawing of a hexamer of wild-type GluDH, viewed down the 2-fold axis, with the 3-fold axis vertical. The N-terminal (I) and the C-terminal (II) domains are labeled; it can be seen that domain I is closest to the 32 symmetry point of the hexamer, with domains II on the periphery of the molecule. The active site cleft can be seen between the two domains.

the subunit can be described as a rigid body rotation of some 14° about an axis lying between the two domains and approximately along the axis of helix α16. This motion has the effect of closing the cleft between the two domains and bringing the C4 of the nicotinamide ring and the Cα of the glutamate substrate into a more appropriate orientation for hydride transfer to occur. This has led us to describe the free enzyme as an open form and the glutamate-bound enzyme as a closed form. In a comparison of the open and closed forms, small changes in the main chain torsion angles are seen in four regions of the polypeptide chain. These areas are thought to be critical components of the hinges that control the domain motion and center on residues 200−206 (the loop between βf and α9), 375−379 (the link between α15a and α15b), 391−394 (the loop between α15b and α16), and 421−423 (the loop between α16 and α17).

Analysis of the K89L,S380V structure shows that the relative orientation of the two domains is more closely related to that of the closed structure than to that of the open form. If the K89L,S380V structure is superimposed onto the structure of the closed form, using the domains I as the equivalenced residues, then the rms deviation between the residues in domain I is 0.65 Å and that in domain II is 3.6 Å. If the mutant enzyme is overlapped in the same way with the wild-type open structure, then the rms deviation between atoms in domain I is 0.79 Å and domain II is 8.6 Å. However, there remains a significant difference between the mutant structure and the closed form, with the two domains even more tightly closed, and compared with the open wild-type structure, the relative domain orientations can be described as a rigid body rotation of some 23° about an axis approximately equivalent to that relating the open and closed structures (Figure 3). Both of the disordered stretches

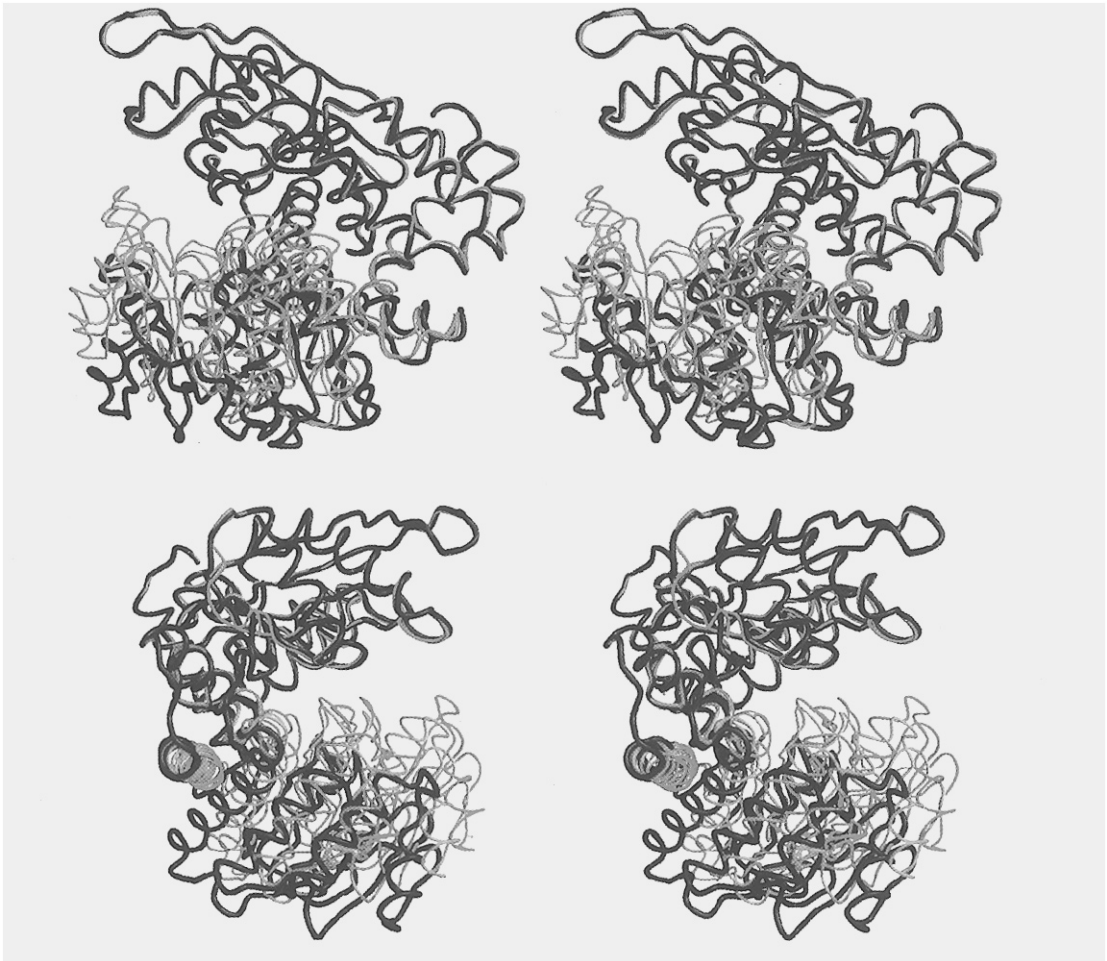

FIGURE 3: Midas (*23*, *24*) stereo representation of the subunit structures of the wild-type open structure (blue), the wild-type glutamate-bound closed structure (red), and the K89L,S380V double mutant structure (green). The structures have been superimposed on the N-terminal domains, and the two views show the cleft closure seen in the different crystal forms of this enzyme.

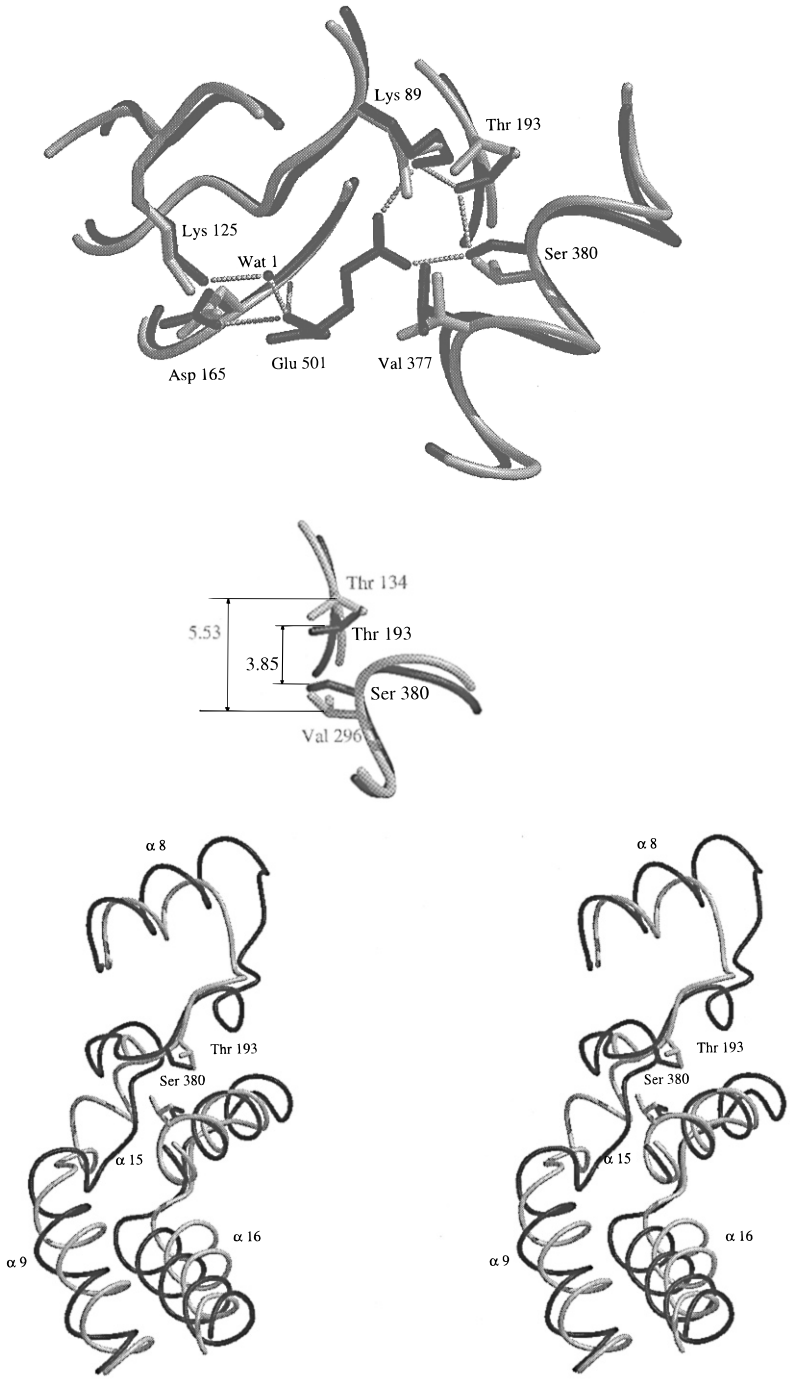

FIGURE 4: Midas representation of the active sites of GluDH (black) and LeuDH (gray) superimposed. (a, top) The glutamate substrate of GluDH is shown (Glu 501), together with important active site residues. The coordinate modification of Lys 89 and Ser 380 in GluDH to leucine and valine, respectively, in LeuDH can be seen. (b, middle) A close-up of (a) showing that the relative distance between the β carbons of T193 and S380 in GluDH is much less (3.85 Å) than that between the equivalent two residues in LeuDH, T134 and V294 (5.53 Å), explaining why no steric clash between these two residues is seen in LeuDH. (c, bottom) A more distant stereoview, showing that the loops preceding and following T134 and the loop after S380 adopt very different conformations in GluDH and LeuDH.

of the polypeptide in the K89L,S380V mutant (193−204 and 383−393) form loops in the wild-type structure which lie adjacent to each other (Figure 1) and form two of the four hinges identified in comparisons of the open and closed forms of the wild-type enzyme. The disruption of these two hinges in the mutant structure will presumably perturb the normal hinge bending of the two domains, thus providing a possible explanation for the poor catalytic efficiency of the mutant.

Substrate Binding. As it seems likely that the disorder of the residues 193−204 and 383−393 is introduced by the mutations, we examined the different structures of GluDH to seek an explanation for this disorder. In the binary complex of the wild-type GluDH with glutamate the side chain of the substrate lies in a pocket on the enzyme surface, with the γ-carboxyl making hydrogen bonds to the side chains of K89 and S380 (Figure 4). The serine residue, S380, lies on helix α15b, and in the open wild-type structure its side chain hydroxyl group is in an appropriate orientation to hydrogen bond to the main chain carbonyl of V377. In the closed wild-type structure, the side chain of this serine adopts a different conformation, allowing it to hydrogen bond to both the side chain of T193 and the side chain carboxyl group of the glutamate substrate. If the mutation made to each of these residues (K89L, S380V) is modeled in turn,

in either the open or closed wild-type structures, then the K89L mutation can be accommodated freely, without any steric clashes. In contrast, the replacement of S380 by valine appears to result in a clash with either the side chain of T193 or the carbonyl oxygen of V377, irrespective of the relative domain orientation. Thus, if the S380V side chain has $\chi_1 = -60°$, then the distance between one of its methyl groups and the carbonyl oxygen of V377 is 2.5 or 2.0 Å (open and closed structures, respectively), whereas in the other two rotamers the separation between one of the methyl groups and the side chain oxygen of T193 is 2.3 and 2.1 Å (open and closed structures, respectively).

In the observed structure of the K89L,S380V double mutant, T193 lies on one of the disordered loops. This strongly supports the idea that the presence of a valine side chain at position 380 results in a severe steric clash with the side chain of T193, which cannot be accommodated within the structural framework of GluDH and results in a breakdown in the order of the polypeptide chain around T193. We assume that the disorder of the loop 193−204 further disrupts the structure by abolishing the interactions between this loop and the 383−393 loop, which lies adjacent to it in the structure, resulting in the associated disorder of this second stretch of polypeptide chain.

It is clear from these results that the active site of GluDH cannot accommodate a valine at position 380 because of the clash with T193. However, the active site of LeuDH contains both residues T134 and V294 (equivalent to T193 and S380V in GluDH), implying that the local structures of GluDH and LeuDH must be subtly different so as to accommodate these sequence differences. The two domains of LeuDH adopt a relative orientation in the crystal even more open than the open form of GluDH (*15*), with one methyl group of the side chain of V294 packing against the carbonyl oxygen of V291. Unlike GluDH, however, in none of the rotamers of the V294 side chain is there a steric clash with the side chain of the adjacent threonine, T134. This difference between GluDH and LeuDH arises from the difference in the relative positions of the α-carbon atoms of T134 and V294 (LeuDH numbering), compared with their counterparts in GluDH. Whereas in LeuDH the separation between these atoms is 6.5 Å, in both the open and closed wild-type GluDH structures the distance between the equivalent α-carbons is only 5.3 Å. The difference in the relative positions of the Cβ atoms of these residues is even greater, being 5.5 Å between Cβ-T134 and Cβ-V294 in LeuDH, compared to 3.8 Å between Cβ-T193 and Cβ-S380 in GluDH (Figure 4).

Why then do these residues adopt different relative positions in LeuDH to that seen in GluDH? The answer appears to be related to the different quaternary structures of these two enzymes. GluDH is a hexamer and LeuDH an octamer, and there are significant differences in the packing of a number of loops in the two structures around their respective 3- and 4-fold axes. The loops that link α8 with βf (the β strand carrying T193), βf with α9, and the loop linking α15b (carrying S380V) to α16 are important in the subunit assembly of GluDH, making intimate interactions around the 3-fold axis. In contrast, there are major differences in the stretches of polypeptide chain which link the equivalent secondary structure elements in LeuDH. The loop preceding the strand carrying T134 in LeuDH (equivalent to T193 in GluDH) and the loop following the helix on which V294 is situated (equivalent to S380V in GluDH) are considerably shorter than the equivalent loops in GluDH, by 9 and 7 residues, respectively. Furthermore, the loop following T134 adopts a substantially different conformation in LeuDH from that seen in GluDH (figure 4). All three of these stretches of polypeptide chain make important interactions around the 4-fold axis in the LeuDH octamer (*15*). While none of these second shell residues contribute directly to the active site, it is the differences in their packing described here which give rise to the modification of the relative distances between the crucial residues responsible for substrate binding.

The initial homology based modeling between GluDH and LeuDH indicated that their differential substrate specificity might be due to a small number of point mutations, which suggested that the rational manipulation of this specificity between members of the family might be accomplished by the creation of a series of simple mutations. This would then open up the way for the construction of a range of designer enzymes with multiple applications in areas of chiral synthesis and diagnostics. However, the results presented here suggest that this is too simplistic a view and that in designing different specificities Nature has had to be far more subtle in creating the necessary active site structures. Thus the small relative differences in the secondary structure elements that carry these side chains in the specificity pocket of LeuDH and GluDH, and which are mediated, in part, by their different quaternary structures, are responsible for controlling the precise alignment of residues in the active site and form a crucial role in the enzymes' specificity. Therefore, in this enzyme superfamily, important determinants of the differential substrate specificity come not only from coordinate substitutions of certain amino acids to change the chemical nature of the substrate binding pocket but also from the subtle changes in the pocket shape that, in this case, arise from changes in interactions associated with the difference in quaternary structure.

ACKNOWLEDGMENT

We thank the staff at the CCLRC Daresbury synchrotron for help with station alignment. The Krebs Institute is a BBSRC-designated Biomolecular Sciences center.

REFERENCES

1. Nagata, S., Tanizawa, K., Esaki, N., Sakamoto, Y., Ohshima, T., Tanaka, H., and Soda, K. (1988) *Biochemistry 27*, 9056−9062.
2. Takada, H., Yoshimura, T., Ohshima, T., Esaki, N., and Soda, K. (1991) *J. Biochem. 109*, 371−376.
3. Britton, K. L., Baker, P. J., Engel, P. C., Rice, D. W., and Stillman, T. J. (1993) *J. Mol. Biol. 234*, 938−945.
4. Syed, S. E.-H., Engel, P. C., and Parker, D. M. (1991) *Biochim. Biophys. Acta 1115*, 123−130.
5. Ohshima, T., Nishida, N., Bakthavatsalam, S., Kataoka, K., Takada, H., Yoshimura, T., Esaki, N., and Soda, K. (1994) *Eur. J. Biochem. 222*, 305−312.
6. Vancura, A., Vancurová, I., Volc, J., Fussey, S. P. M., Flieger, M., Neuzil, J., Marsálec, J., and Bêhal, V. (1988) *J. Gen. Microbiol. 134*, 3213−3219.
7. Priestley, N. D., and Robinson, J. A. (1989) *Biochem. J. 261*, 853−861.
8. Navarrete, R. M., Vara, J. A., and Hutchinson, C. R. (1990) *J. Gen. Microbiol. 136*, 273−281.
9. Asano, Y., Nakazawa, A., Endo, K., Hibino, Y., Ohmori, M., Numao, N., and Kondo, K. (1987) *Eur. J. Biochem. 168*, 153−159.

10. Asano Y., Nakazawa, A., and Endo, K. (1987) *J. Biol. Chem. 262*, 10346−10354.
11. Misono, H., Yonezawa, J., Nagata, S., and Nagasaki, S. (1989) *J. Bacteriol. 171*, 30−36.
12. Ohshima, T., Takada, H., Yoshimura, T., Esaki, N., and Soda, K. (1991) *J. Bacteriol. 173*, 3943−3948.
13. Baker, P. J., Britton, K. L., Engel, P. C., Farrants, G. W., Lilley, K. S., Rice, D. W., and Stillman, T. J. (1992) *Proteins: Struct., Funct., Genet. 12*, 75−86.
14. Stillman, T. J., Baker, P. J., Britton, K. L., and Rice, D. W. (1993) *J. Mol. Biol. 234*, 1131−1139.
15. Baker, P. J., Turnbull, A. P., Sedelnikova, S. E., Stillman, T. J., and Rice, D. W. (1995) *Structure 3*, 693−705.
16. Wang, X., Britton, K. L., Baker, P. J., Martin, S., Rice, D. W., and Engel, P. C. (1995) *Protein Eng. 8*, 147−152.
17. Leslie, A. G. W. (1992) in *Joint CCP4 and ESF-EACBM Newsletter on Protein Crystallography*, No. 26, SERC Daresbury Laboratory, Warrington, U.K.
18. Collaborative Computational Project No. 4 (1994). *Acta Crystallogr. D50*, 760−763.
19. Tronrud, D. E., Ten Eyck, L. F., and Matthews, B. W. (1987) *Acta Crystallogr. A43*, 489−501.
20. Jones, T. A. (1985) *Methods Enzymol. 115*, 157−171.
21. Rossmann, M. G., Moras, D., and Olsen, K. W. (1974) *Nature 250*, 194−199.
22. Kraulis, P. J. (1991) *J. Appl. Crystallogr. 24*, 946−950.
23. Ferrin, T. E., Huang, C. C., Jarvis, L. E., and Langridge, R. (1988) *J. Mol. Graphics 6*, 13−27.
24. Huang, C. C., Pettersen, E. F., Klein, T. E., Ferrin, T. E., and Langridge, R. (1991) *J. Mol. Graphics 9*, 230−236.

BI972024X